Available online at www.sciencedirect.com

SciVerse ScienceDirect

Procedia Engineering 56 (2013) 421 – 428

Procedia Engineering

www.elsevier.com/locate/procedia

5th BSME International Conference on Thermal Engineering

Numerical simulation of slag foaming in high temperature molten metal with population balance modeling

M.A.Sattar*, J.Naser, G.Brooks

Faculty of Engineering and Industrial Science
Swinburne University of Technology
Hawthorn- 3122 Australia

Abstract

A computational fluid dynamic (CFD) model has been developed for the simulation of slag foaming on bath smelting slag (CaO-SiO-Al_2O_3-FeO) by considering foam as a separate phase which is comprised of a mixture of gas and liquid. The model accounts for the formation of foam due to transformation of both gas and liquid into foam and it's destruction due to liquid drainage and bursting of bubble. The bubble break-up and coalescence was considered in gas-liquid dispersion whereas in the foam layer, the bubble coalescence due to film rupture was incorporated. Population balance modelling was used to track the number density of different bubble class. The model predicted the foam height of the slag system (CaO-SiO-Al_2O_3-FeO). The foam height was found to increase with the increase of superficial gas velocity. The content of FeO was changed and its effect on the foaming index was observed. The results from the present model show that foaming index decreases with increase of FeO content in slag. The results from the CFD model also show that the foaming index of a slag with Al_2O_3 is higher than that of slag without Al_2O_3. The predicted results from the present study are in reasonable agreement with the experimental data.

Selection and peer review under responsibility of the Bangladesh Society of Mechanical Engineers

Keywords: Bubble break up; Coalescence; Film rupture; Population balance; CFD.

1. Introduction

Slag foaming phenomena are found in many ferrous and non-ferrous pyrometallurgical processes, such as open hearth furnace, basic oxygen furnace (BOF), blast furnace, and coppermaking. The pyrometallurgical processes generate large quantity of gas which causes slag foaming. Foaming slags are important for post combustion and the large surface areas facilitate the multiphase reactions; leading to improved process kinetics, heat transfer and energy efficiency [1-2]. On the other hand excessive slag foaming can cause the slag to overflow the vessel. This phenomenon is termed as slopping which reduces productivity and increases operating cost and in some cases damages the vessel. Therefore, it is important to understand the features of the slag foaming in the pyrometallurgical processes.

The foaming index, which correlates the foam height with superficial gas velocity, was used for aqueous system [3]. The foaming index has empirically been related to physical properties of the slag such as the surface tension, viscosity, and density of the liquid and the size of the bubbles. Jiang and Fruehan [2] empirically modelled foaming index for different slag foaming. Lahiri and Seetharaman [4] explicitly accounted for the bubble size of the foam. Ito and Fruehan [5] studied the foaming index and foam life to understand the effect of slag composition on foaming in iron and steel making process. The bubble break up model of Luo and Svendsen

* Corresponding author. Tel.: +61424910627; fax: +61 3 9214 8264.
E-mail address: ssattar@swin.edu.au

Selection and peer review under responsibility of the Bangladesh Society of Mechanical Engineers
doi:10.1016/j.proeng.2013.03.142

[6] and the coalescence model of Prince and Blanch [7] are used in the present study. The bubble coalescence model based on film rupture by Tong et al. [8] has been used in the foam layer. The advent of high speed computing machine facilitates the use of computational fluid dynamic model in many engineering fields. Numerous CFD model of multiphase flow have been developed, and numerical data has been validated through comparison with experimental data. It has been successfully used in metal processing involving gas-liquid flow [9-11].

In this study a CFD model based on Euler–Euler approach has been developed to simulate slag foaming. The model predicts the foam height with different superficial gas velocity and iron oxide (FeO) content. The foam was considered as separate phase which is comprised of a mixture of gas and liquid. Different bubble classes were considered and the population balance modeling was incorporated to track the number density of different bubble classes. Bubble break up and bubble coalescence were employed and their Sauter mean diameter were evaluated in the foam. Finally foaming index for different FeO content was determined and elucidated.

2. Mathematical model

2.1. Euler-Euler Multiphase model

The governing equations used in the present study under the Eulerian-Eulerian multiphase approach are summarized in this section. Gas, liquid and foam are treated as separate phases. The CFD solver employed uses the finite volume discretization method which rests on integral conservation statements applied to a general control volume. The Eulerian multiphase flow model solves the conservation of mass and momentum of each phase in each cell. Mass conversion equation used:

$$\frac{\partial \alpha_k \rho_k}{\partial t} + \nabla . \alpha_k \rho_k V_k = \sum_{l=1, l\neq k}^{N} \Gamma_{kl} \ , \quad k=1,\ldots\ldots,N \tag{1}$$

Where α_k is the volume fraction of phase k, $V_k$is phase k velocity, and Γ_{kl} is the interfacial mass exchange between phases k and l. The mass transformation between gas and foam was calculated using the following equation:

$$\Gamma_f = \frac{\pi}{6} d_i^3 (\rho_g \sum_i^n N_{i_g} - \rho_f \sum_i^n N_{i_f}) = -\Gamma_g \qquad N_{i_g} \leq N_{i_{av}} \tag{2}$$

Where N_{i_g} is the number of bubble in gas phase transformed into foam phase, N_{i_f} is the number of bubble in foam transformed into gas phase and $N_{i_{av}}$is the number of gas bubble available in that cell. The number of gas bubble transformed into foam bubble was calculated from the equation.

$$N_{i_g} = \frac{\alpha_l v_c}{n_p a_p l_i} \tag{3}$$

Where α_l is volume fraction of liquid in the cell and v_c is the volume of that cell. The number of foam bubble transformed into gas bubble is calculated from the equation:

$$N_{i_f} = \frac{q_{PB}}{n_p a_p l_i} \tag{4}$$

The liquid drainage due to gravity through plateau border derived by Bhakta and Ruckenstein [12] is used in the present study.

$$q_{PB} = 2N\bar{R}\left(\frac{n_p}{5}\right)\bar{q} = \frac{3}{15} N R n_p a_p u \tag{5}$$

The mass transformation between liquid and foam was calculated using the following equation:

$$\Gamma_f = n_p a_p l_i (\rho_l \sum_i^n N_{i_g} - \rho_f \sum_i^n N_{i_f}) = -\Gamma_l \qquad N_{i_g} \leq N_{i_{av}} \tag{6}$$

Population balance equation has been used as:

$$\frac{\partial}{\partial t} \alpha_k \rho_k \emptyset_{ki} + \nabla . \alpha_k \rho_k V_k \emptyset_{ki} = \nabla . \alpha_k \rho_k D_{ki} \nabla_{\emptyset_{ki}} + S_i \tag{7}$$

Where $S_i = B_{B_i} - D_{B_i} + B_{C_i} - D_{C_i}$ is the source term due to break up and coalescence in the foam and gas-liquid dispersion and $\emptyset_i$ is the fraction of bubble class i . B_{B_i} , B_{C_i} and D_{B_i}, D_{C_i} are birth and death due to break up and coalescence. The source term model of Hagesaether et al. [13] has been used with rectification as:

$$B_{B_i} = \sum_{k=i+1, i\neq N}^{N} \Omega_B(\vartheta_k, \vartheta_i) + \sum_{k=1, i\neq N}^{i} X_{i+1,k}\Omega_B(\vartheta_{i+1}, \vartheta_k), i = 1, \dots\dots, N, \quad (8)$$

$$D_{B_i} = \sum_{k=1}^{i-1} \Omega_B(\vartheta_i, \vartheta_k) + \sum_{k=1, i\neq N}^{i} X_{i,k}\Omega_B(\vartheta_i, \vartheta_k)\ i = 2, \dots\dots, N, \quad (9)$$

$$B_{C_i} = \sum_{j=1, i\neq N}^{i-1} X_{i,j}\Omega_C(\vartheta_i, \vartheta_j) + \sum_{j=1}^{i-1}(1 - X_{i-1,j})\Omega_C(\vartheta_{i-1}, \vartheta_j), i = 2, \dots\dots, N, \quad (10)$$

$$D_{C_i} = \sum_{j=1}^{N-1} \Omega_C(\vartheta_i, \vartheta_j) - \sum_{j=1}^{i} X_{i,j}\Omega_C(\vartheta_i, \vartheta_j), i = 1, \dots\dots, N-1, \quad (11)$$

Where $\Omega_B(\vartheta_k, \vartheta_i)$ is the break-up rate of bubble class k that goes into i and the complementery fraction $v_j = x_{i,k}v_i + (1 - x_{i,k})v_i$ and $x_{i,k} = 2^{1+k-i}, k < i$. The term $\Omega_C(\vartheta_i, \vartheta_j)$ is coalescecne rate of bubble i and j and the colaescence product is distributed as $v_i + v_j = x_{i,j}v_i + (1 - x_{i,j})v_{i+1}$ and $x_{i,j} = 1 - 2^{j-i}, i \geq j$.

2.2. Foam formation and destruction

In foam, bubble bursts at the top and coalesce inside due to film rupture caused by liquid drain-out through the plateau border. It is difficult to incorporate these characteristics of foam in an ordinary two phase gas/liquid simulation approach because the gas diffuses to the atmosphere and is difficult to hold at the top. The above drawback is eliminated by considering foam as a separate phase made up of gas and liquid. The new approach enables us to apply above characteristic of foam. In wet foam the liquid volume fraction is typically between 10% and 30% while in dry foam the volume fraction of liquid is less than 10% [14-16]. In the present study the gas liquid mixture is considered to be foam when the gas volume fraction is more than or equal to 0.75. The gas and liquid transformation mechanism is activated in the model when the gas fraction is 75% or above. However, the amount of gas and liquid transformed into foam and vice versa are governed by equations (20)-(23). That means, gas and liquid will not be transformed into foam just because the criteria of 75% gas in a cell is satisfied. However, in the absence of a proper surface active agent in the foam, the viscosity, density and surface tension properties of foam will be such that the bubble inside the foam will burst immediately and foam will return to liquid and gas phases. A total of 21 scalars were assigned to track 10 bubble classes in gas and 10 bubble classes in foam separately and a liquid in the foam. The density and viscosity of foam is calculated by the following equation:

$$\rho_f = \rho_g + \rho_l(1 - \emptyset) \quad (12)$$

$$\mu_f = \mu_g + \mu_l(1 - \emptyset) \quad (13)$$

Where ρ is density, μ is viscosity $\emptyset$ is liquid fraction in the foam and subscript f, g, l denote foam, gas and liquid respectively. The bubble is considered as pentagonal dodecahedron shape which consists of 12 films and 30 channels. The number of film per bubble is $n_f = 6$ and the number of plateau border channel is $n_p = 10$. The total amount of liquid entrapped per bubble is the sum of the liquid in lamellae and the plateau border. The total amount of liquid $\emptyset_i$ entrapped by the bubble class i is:

$$\emptyset_i = N_i n_p a_p l_i + N_i n_f a_f x_f \quad (14)$$

Where N_i is the number of bubble, l_i is the length of plateau border, a_p is the cross section of the plateau border of bubble class i and x_f is the thickness of the film. The thickness of the film is much smaller, so neglecting the liquid in film $\emptyset_i = N_i n_p a_p l_i$. Total amount of liquid entrapped by all the bubbles in a bubble class is the sum of the liquid entrapped by each individual bubbles in the class.

$$\emptyset = \sum_i^N \emptyset_i \quad (15)$$

The liquid drainage velocity $u = \frac{c_v a_p \rho g}{20\sqrt{3}\mu}$ due to gravity through plateau border derived by Bhakta and Ruckenstein [12] is used in the present model and the cross section of the plateau border is $a_p = 0.161{r_p}^2$.

2.3. Bubble break up and coalescence model

The break up model of Luo and Svendsen [6] was used in the present study. The rate of bubble break up $\Omega_B$is the product of collision frequency ω_B and the probability of bubble break up P_B. The break up rate of bubble class i into j colliding with the eddy size λ_j can be written as:

$$\Omega_B\left(\vartheta_k, \lambda_j, \vartheta_i\right) = \omega_B(d_i, \lambda_j) \times P_B(d_i, \lambda_j, d_k) \tag{16}$$

The coalescence model of Prince and Blanch [6] has been used in the present study. Turbulent collision rate:

$$\theta_{ij}^{T} = 0.089 n_i n_j (d_i + d_j)^2 \varepsilon^{1/3} (d_i^{2/3} + d_j^{2/3})^{1/2} \tag{17}$$

Laminar shear collision rate:

$$\theta_{ij}^{LS} = \frac{4}{3} n_i n_j \left(r_i + r_j\right)^3 \left(\overline{\frac{dU_l}{dR}}\right) \tag{18}$$

The mean shear rate is calculated as:

$$\bar{\gamma}(R) = 5.3 \frac{U_{l,max}}{R_T} \tag{19}$$

Where R_T is the radius of the container, $U_{l,max} = \left(\frac{(1-0.75\alpha_g)}{1-\alpha_g}\right)\frac{\alpha_g g D_T^2}{48\upsilon_t}$ is the centerline liquid circulation velocity and $\upsilon_t = 0.0536\frac{D_T^{1.77}}{\rho_l}$ is the turbulent kinetic viscosity. The coalescence efficiency $P_C\left(r_i, r_j\right) = exp\left[-\frac{\left\{\frac{r_{ij}^3 \rho_l}{16\sigma}\right\}^{1/2} \varepsilon^{1/3} \ln\frac{h_0}{h_f}}{r_{ij}^{2/3}}\right]$ with initial and final thickness for air-water is 1×10^{-4}m and 1×10^{-8}m from Prince and Blanch [6]. The coalescence rate Γ_{ij} of bubble i and j is given by the total collision frequency multiplied by the coalescence efficiency.

$$\Gamma_{ij} = \left\{\theta_{ij}^{T} + \theta_{ij}^{LS}\right\} \times P_C\left(r_i, r_j\right) \tag{20}$$

The coalescence rate $\Omega_{C_{i,j}}^{f}$of a bubble of the ith group with bubbles of the jth group in the foam is [8]:

$$\Omega_{C_{i,j}}^{f} = n_{p_i} P_{i,j} f_{i,j} \tag{21}$$

where n_{p_i} is the number of films per bubble of the ith group, $\mathrm{P_{i,j}} = \mathrm{k}\frac{1}{\tau}$ is the failure rate of films separating bubbles of the ith and jth groups, $f_{i,j} = \frac{n_{p_i} n_i}{\sum_{j=1}^{M} n_{p_j} n_j}$ is the probability of a bubble of the ith group sharing the same film with the bubbles of jth group in the foam. n_i and n_j is the number of bubble of the ith and jth group respectively. Amount of liquid per bubble, $\emptyset_i/d_i$ so the time required to drain out this liquid is $\tau = (\emptyset_i/d_i)/q_{PB}$.The foaming index was calculated using the equation from Ito and Fruehan [5] as:

$$\sum = \frac{H_f}{U_g^S} \tag{22}$$

Where H_f is the foam height (cm) from the liquid surface and $U_g^S$is the superficial gas velocity (cm/s).

3. Model geometry and methodology

The predictions were carried in a container of height 12cm and the diameter of 4.5cm simulating the small scale experimental model of Jiang and Fruehan [2]. Two different grid of the model was generated with a control volume of 207,705 and 150,103. Simulation was performed on both grid using superficial gas velocity of 1cm/s. and it has been verified the convergence of the solution in both cases. No significant differences were observed in the results. Therefore, for all the subsequent simulations, the 150,103 control volumes numerical

mesh was used. The generated grid for the present model is presented in Figure 1. The nozzle with diameter of 1.6mm was placed at centre and 1cm above from the bottom. As no experimental data for the initial bubble diameter issued from the nozzle were available, the Argon (Ar) gas was assumed to enter the calculation domain as bubbles of diameter of 0.5mm. When the flow dynamics and foam height reached a quasi-steady state, the height of foam was measured as the distance between the top surface of the clear liquid and the top surface of the foam. The simulation was performed by commercial CFD solver in AVL FIRE 2009.2 [17], but the full foaming model comprising of eqns. (1)-(22) were incorporated as subroutine written by author in FORTRAN.

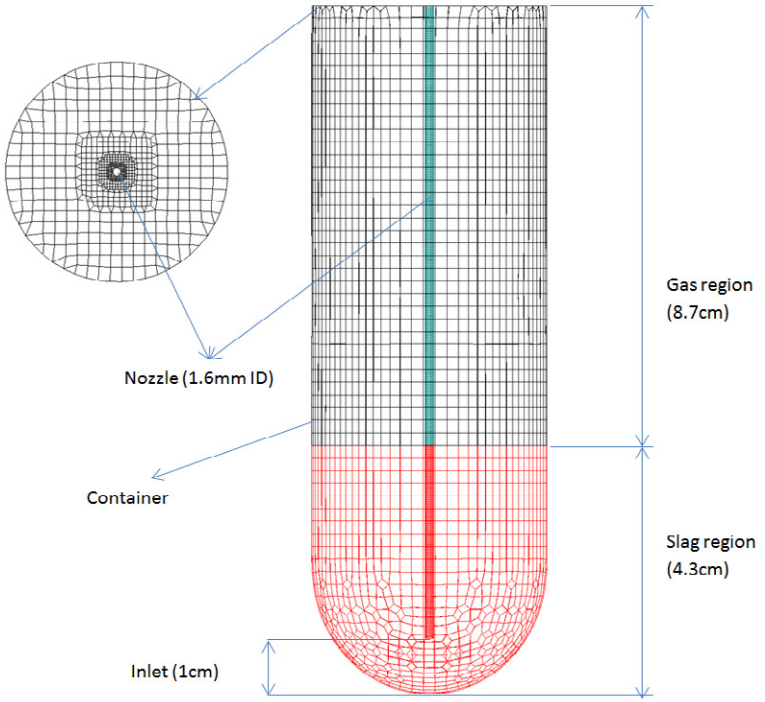

Fig. 1. Grid generated for the simulation

In this model, an unsteady state solution for multiphase momentum and continuity were obtained and for turbulence, a standard $k-\varepsilon$ turbulence model was used. For momentum and turbulence, first order upwind differencing scheme was used whereas central differencing scheme with second order accuracy was used for the continuity equation. The properties of the fluids used in this study are presented in Table 1.

Table 1. The properties of the fluids used.

Properties	Gas(Ar)	Liquid CaO/SiO=1.25, Pct Al_2O_3=4			Foam
		Pct FeO =3.0	Pct FeO =7.5	Pct FeO=15	
Density(kg/m^3)	0.2745	2733	2790	2889	Eq.(12)
Viscosity(Ns/m^2)	2.23E-05	0.381	0.353	0.314	Eq.(13)
Surface tension (mN/M)	-	477.2	483.6	494.6	-

4. Results and discussion

The simulation was carried out in a crucible filled up to 4cm of slag from the bottom. The simulation was run for 300 second of real time. Due to transient flow behaviour, the foam height was in quasi steady state so the average foam heights from 250s to 300s were measured at an interval of 10s. The foam heights at different position were measured and the average height of foam was considered. The instantaneous foaming heights are presented as foam volume fraction for superficial gas velocity of 1, 2 and 3cm/s at 250s in Figure 3.

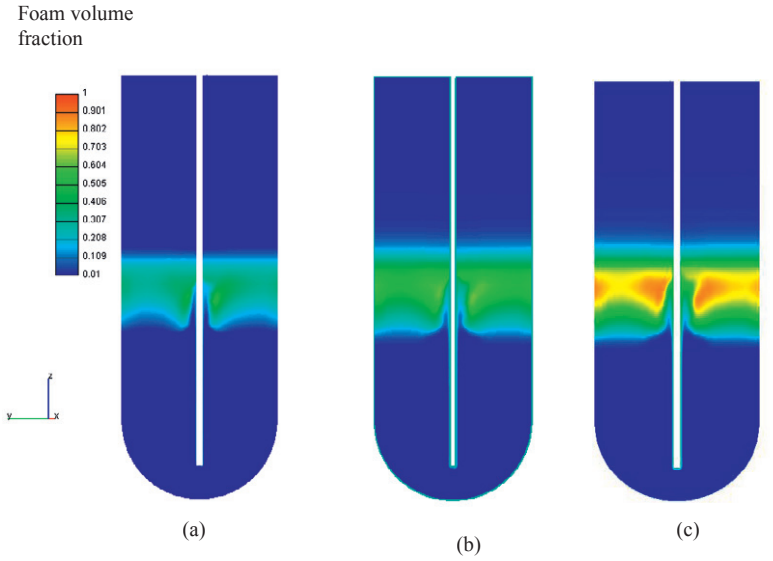

Fig. 2. Slag foam formation at 1773K for 3pct FeO (a) $U_g = 1cm/s$ (b) $U_g = 2cm/s$ (c) $U_g = 3cm/s$.

Different superficial gas velocity was employed for the same composition to achieve accurate foaming index. The foaming height of CaO-SiO-Al_2O_3-FeO slags as a function of superficial gas velocity is shown in Figure 4 along with the data from Jiang and Fruehan [2]. As expected the foaming height increases with the increase of gas flow rate when the slag composition is same.

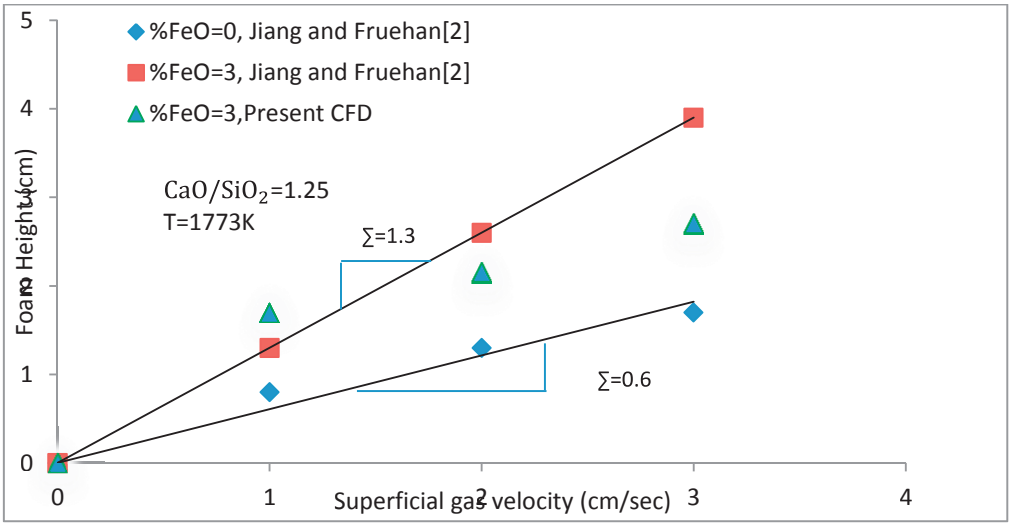

Fig.3. Foam heights of slags with different superficial gas velocity at 1773K.

The height of slag foam depends on the foam formation due to gas flow and destruction due to the bubble burst at the top and the liquid drainage. The liquid drainage through plateau border channel remained same for the same slag composition but the total liquid drainage in the foam increases due to the increases of volume of foam. Bubble burst at the top which remain constant due to constant surface area. For this reason increasing superficial gas velocity causes the increases of foam height when the slag composition is same. The foaming index of the present CFD model was measured as 1.24 from the slope of the Figure 3 for slag with FeO 3pct. The foaming indices from the present CFD and from Jiang and Fruehan [2] as well as the predicted data from Ito and Fruehan [4] are presented in Figure 4.

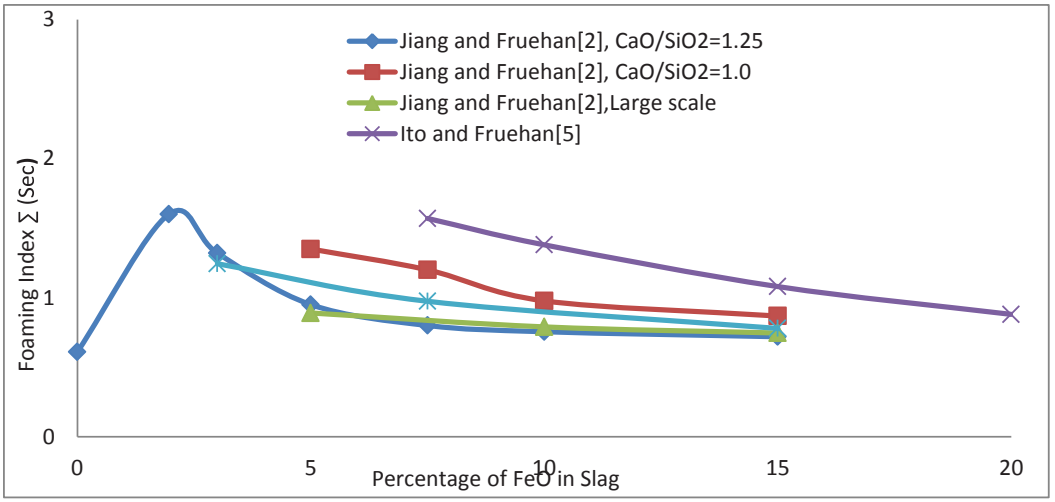

Fig.4. Foaming index of slag with different composition at 1773K.

It can be seen from the Figure 4 that in all cases the foaming index decreases with increase of FeO (For Jiang and Fruehan[2] when pct FeO>2). The foaming index increases with viscosity and is inversely proportional to the square root of surface tension [4]. The net result for these slags is that foaming index decreases with increasing the FeO content (Jiang and Fruehan [2]). The above phenomena can be attributed to the fact that increasing FeO in slag decreases the viscosity of the slag (see Table 1). The drainage of liquid in foam increases with decreases of viscosity. So the height of foam decreases thus decreases the foaming index. The figure also shows that the foaming index of slag with Al_2O_3 is higher than that of slag without Al_2O_3. This is because Al_2O_3 increase the viscosity of slag [2]. The increase of viscosity increases the foaming index as mentioned above. With the 0.5mm diameter of bubble assumed to enter into calculation domain from the nozzle, the Sauter mean diameter calculated in the foam are 0.77mm, 0.85mm and 0.95mm when the FeO content is 3, 7.5 and 15 percent respectively. The above phenomena can be attributed to the fact that increasing FeO in slag decreases the viscosity of the slag (see Table 1). The drainage of liquid in foam increases with the decreases of viscosity. The rate of film rupture increases with the increased drainage causing an increase in the number of upper bubble classes and the Sauter mean diameter.

The results of the present CFD model are in reasonably good agreement with the experimental data of Jiang and Fruehan [2]. The computed foaming index of the present CFD was 5.75% less than that of Jiang and Fruehan [2] when FeO was 3pct. On the other hand the computed foaming indices of the present CFD were 21.77% and 8.35% more than that of Jiang and Fruehan [2] when FeO were 7.5pct and 15pct respectively. The present CFD model assumes that the shape of bubbles during the formation of foam is pentagonal dodecahedron but in reality the bubbles of different shapes exist in the foam. It is also considered in the present simulation that the cross section of the plateau border channel does not change with height of foam and the liquid in the lamellae is negligible compared to the plateau border channel. The life of foam depends on the concentration of surface active agent in the foam. The concentration gradient of the surface active agent in the foam is important for the calculation of drainage and film rupture. At the same time numerical inaccuracy associated with the numerical schemes used in the present study and the turbulence model used in the present study may also have contributed to the inaccuracies in the results. The discrepancies between the results from the present CFD model and that of the experimental data can be attributed to the above mentioned facts. More experiment results based on the above phenomena are necessary to incorporate the physics of foaming in the present CFD model for accurate prediction of the features of foam.

5. Conclusions

In this study a CFD model has been developed for the simulation of slag foaming on bath smelting slag. The results from the present CFD model show that foaming index decreases with increase of FeO content in slag. This phenomenon was attributed to the fact that increasing FeO in slag decreases the viscosity but increases the surface tension. The drainage of liquid in foam increases with the decreases of viscosity resulting in a decrease of foaming index. The results from the CFD model also showed that the foaming index of a slag with Al_2O_3 is higher than that of slag without Al_2O_3.The reason behind this was identified as the increases of viscosity due to

addition of Al_2O_3. The Sauter mean diameter is found to increases with increases of FeO content in slag. This was attributed to the fact that the drainage of liquid in foam increases with the decreases of viscosity. The increased drainage leads to increased rate of film rupture and the number of upper bubble class increases thus causing the Sauter mean diameter to increase. The predicted results from the present study are in reasonably good agreement with the experimental data. The reasons of discrepancies between results of the present CFD model and that of the experimental data were due to the assumptions made to avoid the complexity of simulation and numerical schemes and turbulence model used.

References

[1] Nexhip C, Shouyi S., and Jahanshahi S., 2004. Physicochemical properties of foaming slags. International Materials Reviews 49(5), p.286-298.
[2] Jiang R., and Fruehan R.J.,1991. Slag foaming in bath smelting. Metallurgical and Materials Transactions *B* 22B, p.481-489.
[3] Lahiri A.K., and Seetharaman S.,2002. Foaming Behavior of Slags. Metallurgical and Materials Transactions *B*, 33B, p.499-502.
[4] Bikerman J.J., 1953. Foams: Theory and industrial application, Reinhold Publishing Corporation, New York, NY, p.37

[5] Ito K., and Fruehan R.J.,1989.Study on the Foaming of CaO-SiO2-FeO Slags: Part I. Foaming Parameters and Experimental Results. Metallurgical and Materials Transactions *B* 20B,p.509-14.
[6] Luo H., Svendsen H.F.,1996. Theoretical model for drop and bubble breakup in turbulent dispersions. A.I.Ch.E. Journal42, p.1225-1233.
[7] Prince M.J., Blanch, H.W.,1990. Bubble coalescence and break-up in air-sparged bubble columns. A.I.Ch.E. Journal36, p.1485-1499.
[8] Tong M.K., Cole K., Neethling S.J.,2011. Drainage and stability of 2D foams: Foam behaviour in vertical Hele-Shaw cells. Colloids and Surfaces A: Physicochem. Eng. Aspects 382,p.42–49.
[9] Alam M., Naser J., Brooks G.,2010. Computational Fluid Dynamics Modeling of Supersonic Coherent Jets for Electric Arc Furnace Steelmaking Process. Metallurgical and Materials Transactions B 41b,p.1354-1367.
[10] Alam M., Naser J., Brooks G., Fontana A.,2012. Computational Fluid Dynamics Model of Shrouded Supersonic Jet Impingement on a Water Surface. ISIJ International 52(6).
[11] Huda N., Naser J., Brooks G., Reuter M., Matusewicz R., 2011. Computational Fluid Dynamic Modeling of Zinc Slag Fuming Process in Top-Submerged Lance Smelting Furnace.Metallurgical and Materials Transactions BDOI: 10.1007/s11663-011-9558-6, 2011
[12] Bhakta A., Ruckenstein E.,1997. Decay of standing foams drainage coalescence and collapse. Advances in Colloid and Interface Science70, p.1-124.
[13] Hagesaether L., Jakobsen H.A., Svendsen H.F.,2002. A model for turbulent binary breakup of dispersed fluid particles. Chemical Engineering Science57(16),p.3251-3267.
[14] Pawlat J., Hayashi N., Ihara S., Satoh S., Yamabe C., Pollo. I.,2004. Foaming column with a dielectric covered plate-to-metal plate electrode as an oxidants' generator. Advance in Environmental Research8,p.351-358.
[15] Pilon L., Viskanta R., 2004. Minimum superficial gas velocity for onset of foaming. Chemical Engineering and Processing43, p.149-160.
[16] Drenckhan W., Langevin D., 2010. Monodisperse foams in one to three dimensions. Current Opinion in Colloid & Interface Science15, p.341-358.
[17] AVL FIRE v2009.2. AVL LIST GmbH, Graz, Austria.